1862

RIGA TECHNICAL UNIVERSITY

**Mārcis Eimanis**

# USAGE OF DOUBLE-HELICAL PROPULSION PRINCIPLE IN UNDERWATER VEHICLES

Summary of the Doctoral Thesis

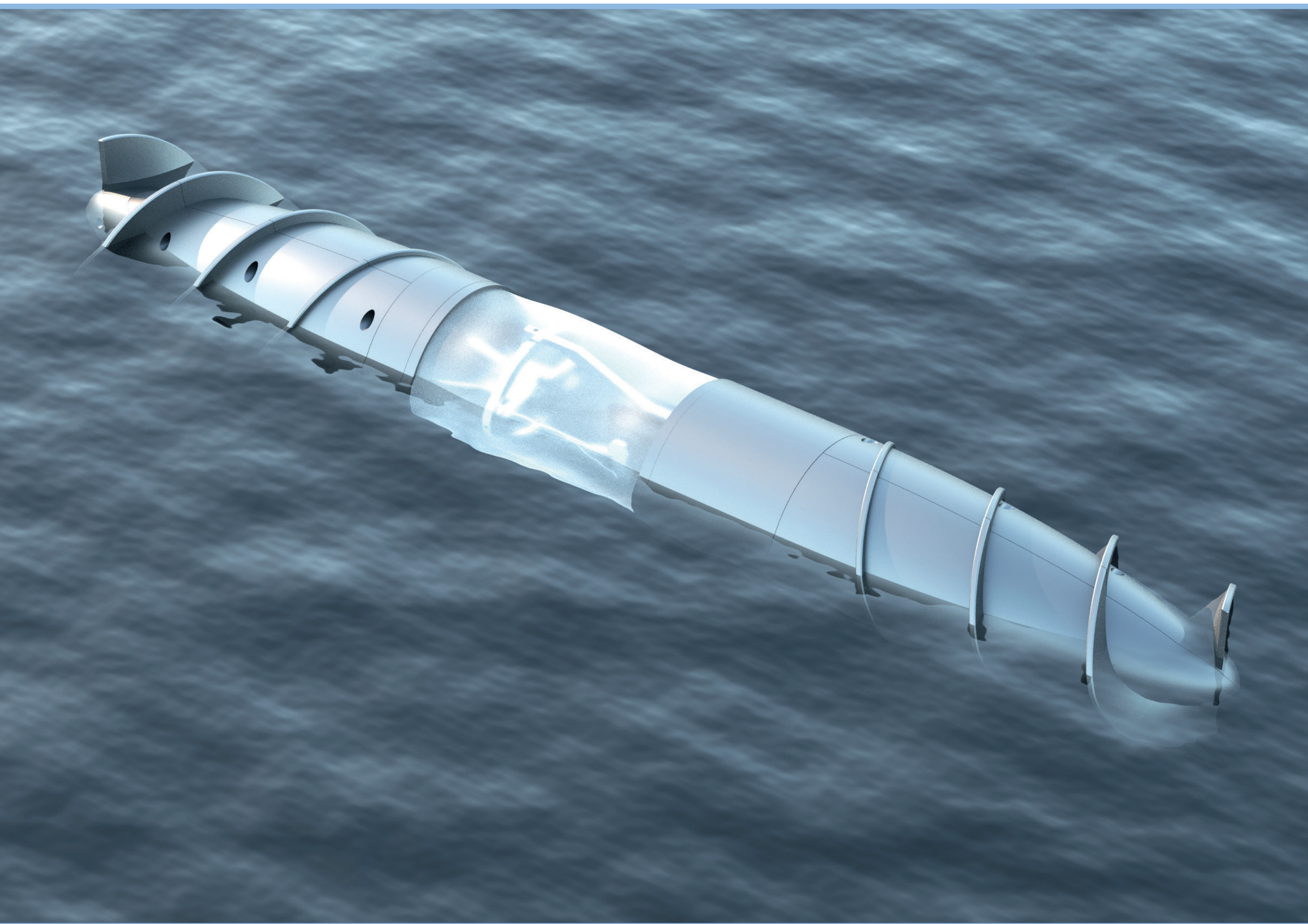

RTU Press
Riga 2022

**RIGA TECHNICAL UNIVERSITY**
Faculty of Mechanical Engineering, Transport and Aeronautics
Institute of Mechanics and Mechanical Engineering

**Mārcis Eimanis**
Doctoral Student of the Study Programme "Engineering Technology, Mechanics and Mechanical Engineering"

# USAGE OF DOUBLE-HELICAL PROPULSION PRINCIPLE IN UNDERWATER VEHICLES

**Summary of the Doctoral Thesis**

Scientific supervisor
Professor Dr. sc. ing.
JĀNIS AUZIŅŠ

RTU Press
Riga 2022

Eimanis, M. Usage of Double-Helical Propulsion Principle in Underwater Vehicles. Summary of the Doctoral Thesis. – Riga: RTU Press, 2022. – 35 p.

Published in accordance with the decision of RTU Promotion Council “P-04” of 1 December 2021, Minutes No. 49.

Cover picture by Mārcis Eimanis

https://doi.org/10.7250/9789934227370
ISBN 978-9934-22-737-0

# DOCTORAL THESIS PROPOSED TO RIGA TECHNICAL UNIVERSITY FOR THE PROMOTION TO THE SCIENTIFIC DEGREE OF DOCTOR OF SCIENCE

To be granted the scientific degree of Doctor of Science (Ph. D.), the present Doctoral Thesis has been submitted for the defence at the open meeting of RTU Promotion Council on 10 March 2022 at the Faculty of Mechanical Engineering, Transport and Aeronautics of Riga Technical University, 6B Kipsalas Street, Room 521.

OFFICIAL REVIEWERS

Professor Dr. sc. ing. Andrejs Krasņikovs
Riga Technical University

Professor Dr. Giedrius Janušas
Kaunas University of Technology, Lithuania

Associate Professor Dr. Sc. D. Gabriel David Weymouth
University of Southampton, UK

DECLARATION OF ACADEMIC INTEGRITY

I hereby declare that the Doctoral Thesis submitted for the review to Riga Technical University for the promotion to the scientific degree of Doctor of Science (Ph. D.) is my own. I confirm that this Doctoral Thesis had not been submitted to any other university for the promotion to a scientific degree.

Mārcis Eimanis……………………………. (signature)

Date: ………………………

The Doctoral Thesis has been written in Latvian. It consists of Introduction, 8 chapters, Conclusions, 113 figures, 4 tables, 2 appendices; the total number of pages is 132. The Bibliography contains 97 titles.

# ANNOTATION

The Thesis describes a new underwater vehicle propulsion type developed by the author. Flow and vehicle interaction dynamics are studied, and factors impacting the flow, control methods and the ability to move in other media (in addition to fluid) are reviewed. A geometry of the propulsion system was created by studying its hydrodynamic properties using a special CFD software. A mathematical model for the control system was created. The dynamics of the underwater vehicle were modelled with the multibody dynamics modelling software *MSC Adams*, using the developed control system and the water resistance model developed with CFD software. Flow dynamics were combined with multibody mechanism dynamics using the metamodeling and numerical experiment approach. Numerical experiments in bulk or granular media were performed using the discrete element method, simulating the vehicle movement using the *EDEM* software. Within the framework of the Thesis, a prototype of the model was also created for observing the model behaviour in real-life conditions. High-quality and good fit results were obtained from the mathematical model and the physical prototype dynamics, proving the performance of both the new propulsion principle and the control system.

# CONTENTS

# GENERAL DESCRIPTION OF THE THESIS

## Relevance

Currently we use many types of propulsion for underwater vehicles and for vehicles moving on the water surface, but the propeller propulsion is still the most popular. Propeller propulsion is used for ships, boats, submariners and torpedoes. Part of these vehicles are also propelled by a water jet propulsion that is also created by a propeller. Each of these types of propulsion has its advantages and disadvantages, but propellers are the most frequent choice. This work reviews different types of water vehicles, their propulsion types, technical solutions and applications.

The same popular propeller-type propulsion is also used for autonomous underwater vehicles (AUV). This type of vehicle is built in such a way that it functions without the direct intervention of a human, using special control systems that operate according to previously defined algorithms. Usually AUVs are used in dangerous environments or to study places that are difficult (often impossible) to access for humans. Given that these vehicles operate according to the laws of non-linear dynamics, they do not have concretized models and face difficulties that are hard to identify and predict. Such vehicles have difficult control system design problems. It is also frequently impossible to comprehensively describe the hydrodynamic ratios, causing unmeasurable complications due to streams [1]. All these problems make it difficult to select an AUV; however, despite all of the aforementioned difficulties, such vehicles are being constructed, improved, and used both in research and in industry.

The propulsion scheme is created by body parts equipped with threads and rotating in opposite directions. They allow the object to "drill" through water, while the flexible middle part allows it to change direction. The invention was inspired by bacteria that use rotating flagella for movement. However, the scheme proposed here is different in that the rotation movement is also performed by the front body, creating positive propulsive force. This type of construction could be used for autonomous underwater vehicles. Previously similar bodies – only with worm gear type propellers placed in parallel – were used for amphibious vehicles [2], but due to the significant disruption of the soil layer the propulsion did not become popular.

## Purpose of the research and main tasks

The purpose of the research is to study the application of the double-helical propulsion principle in underwater vehicles and to prove that such a system can function and can be controlled. In order to achieve this goal, the following main tasks need to be solved:

1. Conducting an analysis of literature on the types of propulsion for AUVs (autonomous underwater vehicles), their mathematical models, analysis methods and software.
2. Creating a model for CFD (*computational fluid dynamics*) software in order to model the forces created by liquid flow and conducting numerical experiments.

3. Creating a simplified liquid resistance model on the basis of the numerical experiments for use in the multibody dynamics modelling software *MSC Adams*.
4. Modelling an AUV based on the double-helical propulsion principle in *MSC Adams*.
5. Developing a PD controller type model for controlling an AUV based on the double-helical propulsion principle.
6. Modelling target tracing dynamics in *MSC Adams*.
7. Creating a model of an AUV based on the double-helical propulsion principle for the discrete element software *EDEMS* and using it to perform numerical experiments in a granular environment.
8. Creating a prototype of an AUV based on the double-helical propulsion principle: design using the *SolidWorks* software and preparation of the more complex elements using modern production technologies, for example, 3D printing.
9. Conducting experiments with the prototype and validating modeling results.
10. Making conclusions and defining the directions for further work.

## Research hypotheses and assumptions

1. It is assumed that the double-helical propulsion principle is new – it has not been described in scientific literature and has not currently been implemented technically, it is usable, controllable and efficient.
2. It is assumed that water is an incompressible liquid, the interaction between water and the mechanism elements takes place in the form of form resistance and surface friction forces.
3. It is assumed that the double-helical propulsion system exceeds the Reynolds number limit defined for such a system, therefore creating a turbulent flow.
4. It is assumed that modern CFD software can be used to obtain approximated water resistance models or metamodels that could be used in a multibody mechanics dynamics software that creates Newton-Euler dynamics models using the description of the mechanism's kinematic scheme.
5. It is assumed that the discrete element method and the corresponding software are capable of sufficiently precisely describing the interaction of particles in bulk media among themselves and with the elements of the mechanism.

## Novelty of the research

The Thesis reviews current and new underwater vehicles and robots, their different models, not limited to the propulsion force created by propellers. The proposed double helicoid propulsion principle also is completely new, innovative, and its constructive solution has not been previously technically implemented. The development of the propulsion was inspired by nature, more specifically, bacteria, therefore the biomimicry methods have also been employed.

The results were obtained using modern, commercially available software that allows reviewing results in space and time. In order to create a more complete mathematical model, the different software was combined, using metamodeling and response surface methods. CFD software was used for determining fluid interaction, the data obtained were then used for creating a model in the multibody simulation software *MSC Adams*.

## Practical application of the research

1. The double helicoid propulsion principle may be used in autonomous underwater vehicles, that could implement different operations in environments that are difficult or even dangerous for human beings, from environmental monitoring to collecting samples from drilling performed by the vehicle itself in the river bed.
2. The constructive implementation also allows moving through pipes, for example, in order to diagnose obstructions and clean them. Thanks to the symmetrical design, the vehicle does not need to turn around in order to travel back.
3. In micro-sizes a device using the double helicoid propulsion principle could travel through the blood vessels of humans or animals in order to perform medical manipulation or deliver medicine to a specific problem location.
4. The amphibious properties of the vehicle allow it to create propulsive force and move in bulk solid or granular media. When equipped with the necessary sensors, it could move, for example, through a grain storage container, implementing internal monitoring. It could similarly be applied for rescue work in rock or snow landslides to find casualties.
5. A specially configured vehicle with the double helicoid propulsion principle also has potential for digging underground ducts for cable lines.

## Thesis approbation

Reviewed scientific articles published in scientific journals with editorial staff in Latvia or abroad, including in university publications:

1. **Eimanis M.**, Auzins J. Method and Device for Production of Driving Force in Underwater Floating Vehicle. *Recent Patents on Mechanical Engineering*, 2021, Vol. 14(2), pp. 175–183, ISSN: 2212-7976, DOI: 10.2174/2212797613999200930163030.

Publications in conference materials indexed in Web of Science and/or SCOPUS:

1. **Eimanis, M.**, Auziņš, J. Research of the Dynamics of Double Helicoidal Vehicle in Granular Media. No: 18th International Scientific Conference "*Engineering for Rural Development*": Proceedings. Vol. 18, Latvia, Jelgava, 22–24 May 2019. Jelgava: LLU, 2019, pp. 1205–1209. ISSN 1691-5976. Available: doi:10.22616/ERDev2019.18.N358.
2. **Eimanis, M.**, Auziņš, J. Flow Analysis of New Type Propulsion System for UVs. No: IOP Conference Series: *Materials Science and Engineering, Latvia*, Riga, 27–29

September 2017. UK: IOP Publishing, 2017, pp. 1–9. ISSN 1757-8981. e-ISSN 1757-899X. Available: doi:10.1088/1757-899X/251/1/012059.

3. Auziņš, J., **Eimanis, M.** Dynamical Simulation and Optimization of Double-Helical AUV. No: MARINE 2015: *Computational Methods in Marine Engineering VI*, Italy, Rome, 15–17 June 2015. Barcelona: International Center for Numerical Methods in Engineering (CIMNE), 2015, pp. 1128–1139. ISBN 978-84-943928-6-3.

Other publications in conference (including local) reports:

1. **Eimanis, M.**, Auziņš, J. Flagella Inspired Propulsion for AUVs. No: *10th Symposium on High-Performance Marine Vehicles HIPER'16*, Italy, Cortona, 17–19 October 2016. Cortona: 2016, pp. 342–354.
2. **Eimanis, M.**, Auziņš, J. Jauna veida zemūdens transportlīdzekļu piedziņas izstrāde. No: *Teorētiskā mehānika: 53. RTU studentu zinātniskās un tehniskās konferences rakstu krājums*. Rīga: RTU Izdevniecība, 2012, 311. lpp. ISBN 978-9934-10-380-3.

Patents:

1. LV15296B, Jānis Auziņš, **Mārcis Eimanis**, Vitālijs Beresņevičs, Guntis Kuļikovskis. IERĪCE UN PAŅĒMIENS ZEMŪDENS PELDLĪDZEKĻA DZINĒJSPĒKA RADĪŠANAI. Granted on 20.03.2018.
2. LVP2021000027, Jānis Auziņš, **Mārcis Eimanis**. IERĪCE UN PAŅĒMIENS, KAS RADA DZINĒJSPĒKU GRANULĀRĀ VAI IRDENĀ CIETVIELU VIDĒ. Submitted on 05.05.2021.

Participation in international conferences with presentations:

1. Engineering for Rural Development 2019. International Scientific Conference 22–24 May 2019. Jelgava, Latvia.
2. 3rd International Conference on Innovative Materials, Structures and Technologies (IMST 2017) 27–29 September 2017, Riga, Latvia.
3. 10th Symposium on High-Performance Marine Vehicles – "Technologies for the Ship of the Future" (HIPER'16), 17–19 October 2016, Cortona, Italy.

Awards:

1. Third place and award in the 6$^{th}$ International Invention and Innovation Exhibition "MINOX 2016", 7–8 October 2016.

# 1. DESCRIPTION OF THE NEW PROPULSION PRINCIPLE

The researchers studied microbiological organisms, including salmonella bacteria, which were determined to have a rotation drive. For *Escherichia coli (E. coli*) and *Salmonella typhimurium* bacteria, the drive flagella rotate 18 000 rpm (Fig. 1.1.) pushing them forward with a speed of 30 μm/s.

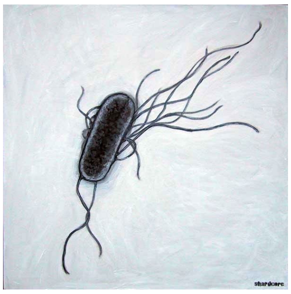
(a)

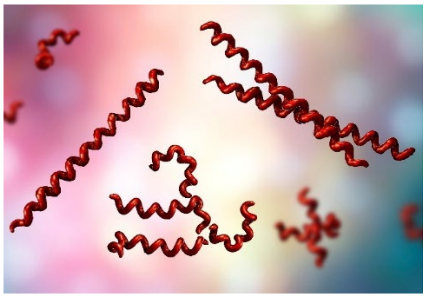
(b)

Fig. 1.1. (a) – *Escherichia coli* bacteria with flagella (left) [3]; (b) – spiral-form bacteria *Spirochaetes* (right) [4].

Within the framework of this research, a new type of underwater vehicle guided propulsion was modelled and created on the basis of the principle of action and reaction. The drive is based on a threaded body that in principle acts similarly to a propeller. The studied type of propulsion has been named *helical drive or helicoid,* in reference to the Greek term *helico-,* meaning "spiral" (i.e., spiral-type drive). The vehicle with this type of propulsion has been named **Durbis**.

In creating the propulsion for Durbis, the principle of biomimicry has been employed – an object found in nature is simulated using multi-disciplinary activities in order to solve a complex engineering problem [5], [6], namely, the inspiration for the propulsion comes from bacteria, *E.Coli* and *Spirochaetes* shown in Fig. 1.1.

The model is planned as an autonomous unmanned device that is not negatively affected by the fact that all of its parts are rotating. This autonomous underwater device has been named "double-helicoid autonomous underwater vehicle", or DHAUV. The Durbis model can be seen in Fig. 1.2.

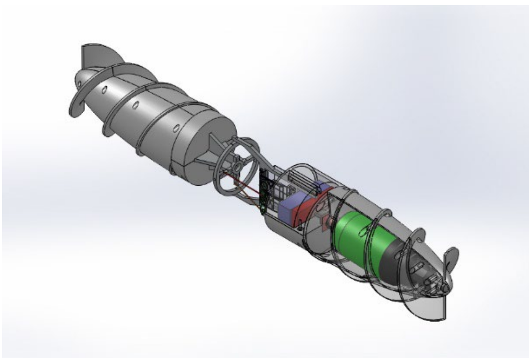

Fig. 1.2. Durbis shown in the *SolidWorks* software.

# 2. REVIEW OF AUTONOMOUS UNDERWATER VEHICLES

Similarly to Durbis, the inspiration for other autonomous underwater vehicles (AUV) often comes from organisms in nature. This section reviews various UVTs that have been developed or are currently in development.

Inspiration from the underwater animal world was most directly used by scientists from the Osaka University in Japan who are developing an underwater robot whose form and construction is inspired by squids. The robot (Fig. 2.1) in general is flat, with fins placed on the sides that create the propulsion force through a wave-like motion [7].

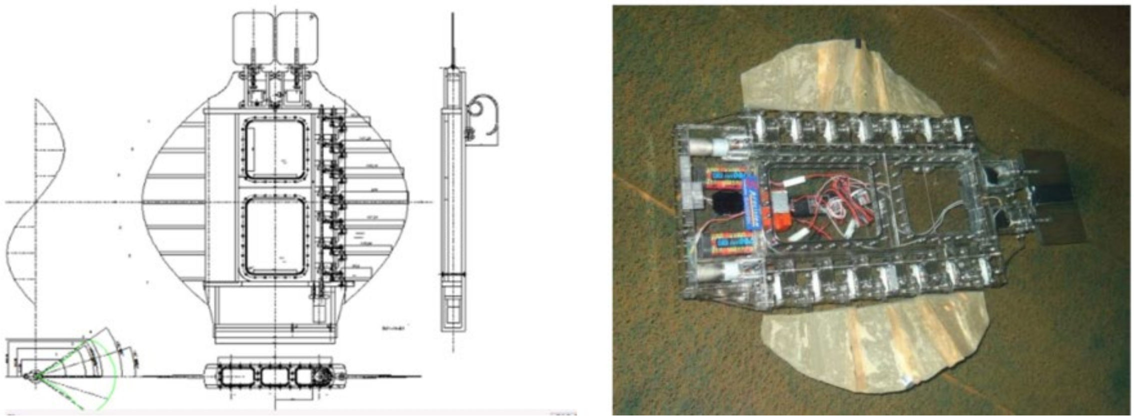

Fig. 2.1. Squid-type robot and its schematic representation [7].

The mechanism that allows the fin to create propulsion force operates according to the 2 dimension wave-like motion law. Assuming that the wavelength is ⅓ m, with a frequency 1 Hz, the equation is:

$$y = 0.05\sin(2\pi kx - 2\pi ft) = 0.05\sin 2\pi k(x - ct), \quad (2.1)$$

where *x* is the coordinate of direction of fin's length; *y* is vertical displacement; *k* is the number of waves 3 1/m; *f* is frequency 1 Hz; and *c* is the wave phase speed ⅓ m/s.

Several experiments have been carried out with the robot, testing its performance, as well as verifying the correspondence of the mathematical model to the natural experiments. For example, one of the experiments tested braking power. Here, as seen in Fig. 2.2, as well as in other experiments, the data show good results – for example, the robot is capable of quickly stopping and changing direction [7].

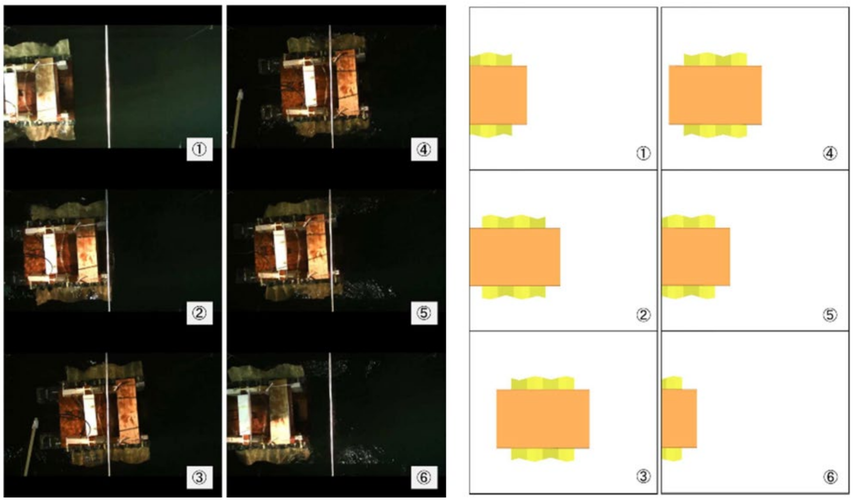

Fig. 2.2. Comparison of the robot's stopping power with the mathematical model (fin frequency 0.75 Hz) [7].

The researchers in the Southampton University in the United Kingdom studied several submerged bodies that radically change their form in order to generate fluid forces. This includes relatively simple form changes, for example, rapid change of fin/wing direction in order to immediately stop, or wings flapped in tandem that create a propulsion force on average three times greater than the force obtained from flapping a single wing. But the experiments also included less traditional form changes, for example, bodies that extremely rapidly contract in order to execute turning or diving maneuvers.

An example from nature that uses a similar a method is the cephalopods (squids, octopuses). They significantly increase their size by filling themselves with water until they project it outwards creating a strong reactive jet, as well as reducing their size, allowing them to rapidly escape from their current location [8]. Vehicles similar to the octopus, created on the basis of soft tissue robotics, at the outflow point usually contract from a spherical form to a 5:1 ellipsoid. Acceleration for such objects is calculated with the following equation:

$$\ddot{x} = \frac{F - \dot{m}U_J}{m} = \frac{\sum F}{m}, \qquad (2.2)$$

where $\Sigma F$ is the total force, namely, the fluid force plus the jet propulsion force $T_J = -\dot{m}U_J$; $-\dot{m}$ is the mass reduction speed and $U_J$ is the jet discharge speed [5].

The simulation results showed that such bodies may attain speeds exceeding $3.5U_J$. Figure 2.3 (a) shows the prototype of this vehicle that is created from a soft membrane and an embedded stiff structure. Similarly to the shell of an octopus, this membrane may be filled with a liquid, forcing it to assume an initially large, blunt form, thereby preserving a sufficient amount of energy to achieve the sudden escape.

Figure 2.3 shows the rapid self-driven acceleration of this robot and the discharge. The speed exceeds 10 L/s or 2.7 m/s approximately $t$ = 0.95 s after launch [9].

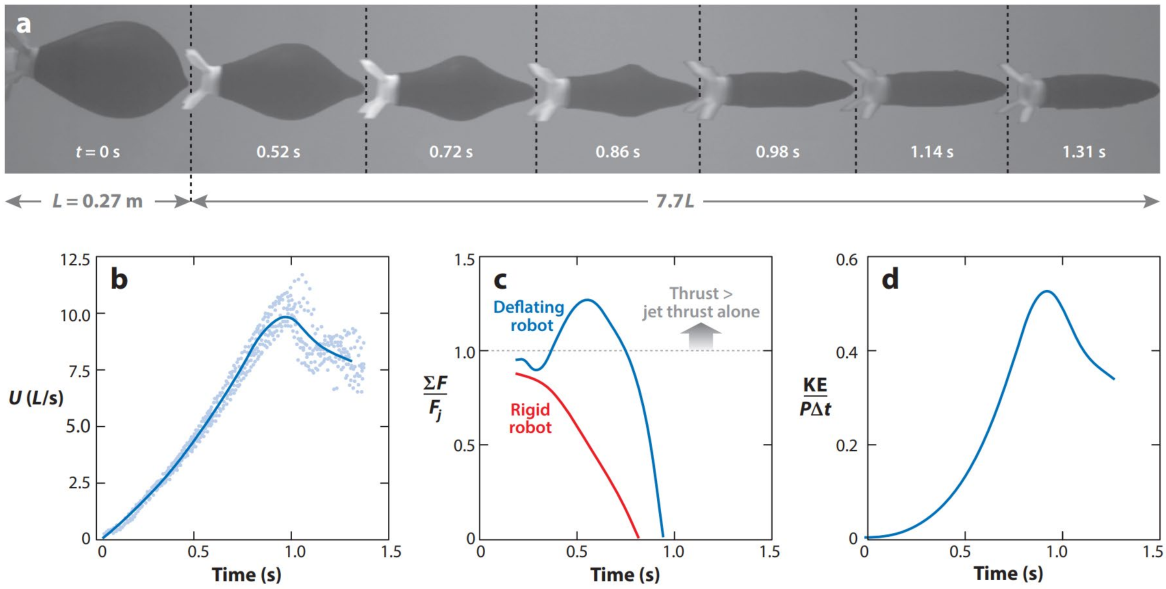


Fig. 2.3. Results of the octopus-like vehicle after the self-propulsion test [10].

The vehicle described above shares a very significant characteristic with Durbis – the propulsion force is generated by the body of the vehicle itself. And, as can be seen here, this method allows obtaining significant results that include both energy efficiency and dynamic performance.

The FILOSE project (in which the Mechanics Institute of the Riga Technical University participated) included the development of a robotic fish with a rubberized tail part (Fig. 2.4). The form of the robot resembles a rainbow trout. As before, the body itself performs the function of generating propulsion force, at least 2/3 of it – the front part (head) is made of a hard material that houses the control system, while the tail part is flexible and uses a servomotor mechanism placed in the thorax to make wave-like motions, generating propulsion force for moving in water [11].

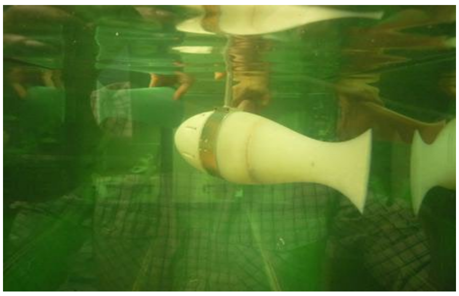

Fig. 2.4. FILOSE robot fish prototype [11].

A rather simple, two-blade propeller drives the AZT *Explorer* (Fig. 2.5), developed by company *ISE (International Submarine Engineering Ltd.)*. This is one of the most traditional types of AUVs currently available, and it is used in industry. The wet cargo compartments with a diameter of 69 cm can hold a broad range of side scanning sonars, as well as multi-beam acoustic scanners and many other tools for determining water column parameters [12], [13].


Fig. 2.5. *ISE Explorer* autonomous underwater vehicle [13].

# 3. CREATING THE MATHEMATICAL MODEL AND ANALYSING IT IN THE *MSC ADAMS* SOFTWARE

## 3.1. Model geometry

In order to analyse the behaviour of the Durbis geometry with a flexible middle body, a mathematical model was created in the *MSC Adams* software, shown in Fig. 3.1. The thread geometry itself was previously created and imported in the *SolidWorks* software.

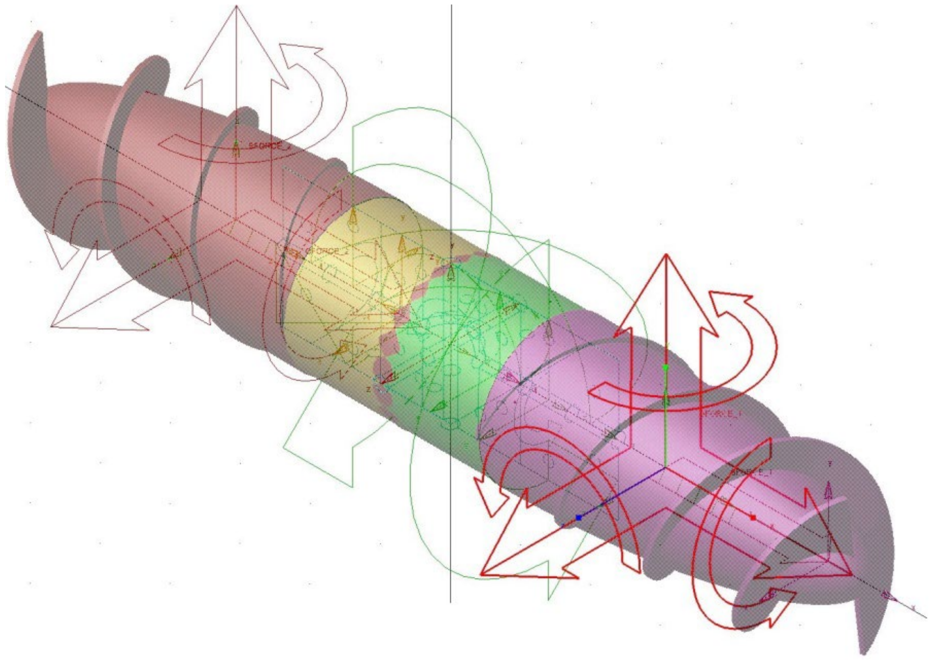

Fig. 3.1. *MSC Adams* mathematical model.

It has been created so that it would have the same degrees of freedom as the planned model. The middle body consists of a sphere and two cylinders that are connected with each other with moving pivots. Threaded bodies are attached to the cylinders that can perform the same rotation that is planned for the real mechanism. Accordingly, the model has 10 degrees of freedom. In order to verify the control principle, a water resistance metamodel [14] was created, assuming that the vehicle components (middle part, bow, and stern) are subject to resistance forces and moments that are proportional to the square of the linear and angular speed. The corresponding values for the resistance coefficients were determined using the *Flow3D* software with the components of Durbis fixed in the flow. The model was created only for the purpose of verifying the performance and maneuvering capacity of the vehicle. The following parameters were not taken into account:

- the effect of added mass;
- surface friction;
- changes of the flow on the read body while the vehicle is in a bent state.

## 3.2. A simplified water resistance model for the DHAUV system

Further we will describe a simplified water resistance model for the DHAUV system. Each DHAUV component is subjected to a torque that can be expressed as

$$T = K_T \cdot \rho \cdot n^2 \cdot D^4, \tag{3.1}$$

where

$K_T$ – propulsion force coefficient;

ρ – water density (kg/m$^3$);

*n* – rotation frequency (rpm);

*D* – thread diameter (m).

After transformation, this equation can be written down as

$$T = k \cdot \omega, \tag{3.2}$$

where $k$ is resistance force coefficient; and ω is rotation speed (rad/s).

After assigning coefficients to the bodies: 1 – bow, 2 – middle body, 3 – stern, an *x, y, z* coordinate system is set up for each part with the corresponding coefficient, replaced by *i*. We obtain the following:

$$\begin{aligned} TF_{xi} &= K_{Txi} \cdot \omega_{xi}^2 = K_{Txi} \cdot \omega_{xi} \cdot \|\omega_{xi}\| \\ TF_{yi} &= K_{Tyi} \cdot \omega_{yi}^2 = K_{Tyi} \cdot \omega_{yi} \cdot \|\omega_{yi}\| \\ TF_{zi} &= K_{Tzi} \cdot \omega_{zi}^2 = K_{Tzi} \cdot \omega_{zi} \cdot \|\omega_{zi}\| \end{aligned} \tag{3.3}$$

The resistance force on the bodies can be expressed similarly:

$$F = k \cdot v^2 = k \cdot v \cdot \|v\| \tag{3.4}$$

(3.4.) after expanding in the coordinate system:

$$\begin{aligned} F_{xi} &= k_{xi} \cdot v_{xi}^2 = k_{xi} \cdot v_{xi} \cdot \|v_{xi}\| \\ F_{yi} &= k_{yi} \cdot v_{yi}^2 = k_{yi} \cdot v_{yi} \cdot \|v_{yi}\| \\ F_{zi} &= k_{zi} \cdot v_{zi}^2 = k_{zi} \cdot v_{zi} \cdot \|v_{zi}\| \end{aligned} \tag{3.5}$$

In the longitudinal direction, the *x* axis is operative, while the *y* and *z* axis components are equal, since the bodies are symmetrical. The equations allow to conclude that 4 coefficients are required: for the resistance force and torque in the longitudinal and perpendicular direction. For the bow and stern part these coefficients are the same. Two additional coefficients are required for the middle part. These coefficients may be determined using flow dynamics simulation in the *Flow3D* software.

## 3.3. Creating the flow resistance model

As mentioned earlier, we used a flow resistance metamodel obtained through numerical experiments where the movement speed and angular speed vectors are projected on a moving coordinate system. These projections on the bow are shown in Fig. 3.2. Analogous equations were also created for the rear body.

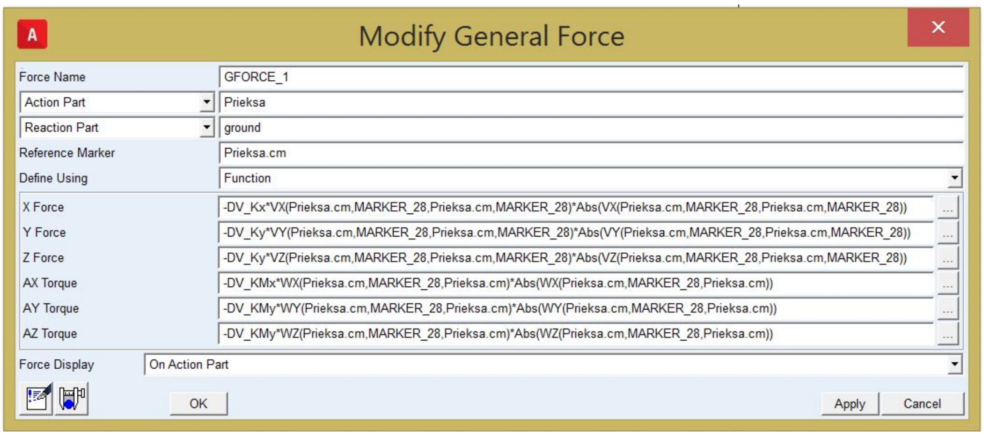


Fig. 3.2. Force projections of the flow metamodel on the vehicle bow.

The equations include resistance coefficients calculated using *Flow3D*. They are resistance force coefficients that are proportional to the square of the speed and were obtained by modelling a rotating Durbis that was fixed in the flow in a stationary position. Different flow speeds and Durbis orientations were used. In order to keep the model from becoming excessively complex, effects from the Durbis bending were not taken into account (for the time being). In this flow resistance metamodel, components of forces and moment reactions in the longitudinal direction were the most relevant. In order to assume that the modelled movement is equivalent to the vehicle swimming with constant propulsion moments $q_1 = q_2 = Q$, it is necessary that the sum of reaction forces in the longitudinal direction is equal to zero (see Fig. 3.3.):

$$R_{x1} + R_{x2} + R_{x3} = 0 \qquad (3.6)$$

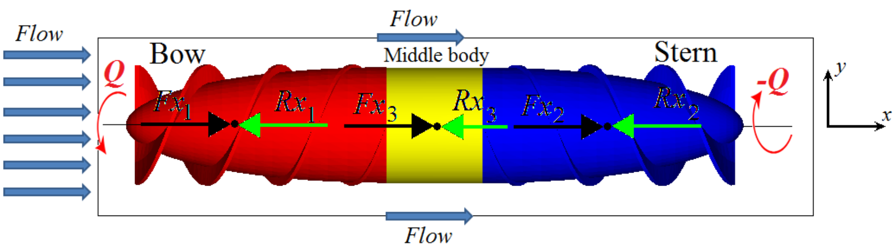


Fig. 3.3. Durbis in finite volume calculation domain, view from above in the *Flow3D* software.

Figures 3.4 and 3.5 show fluid flow lines and horizontal flow speed contours for the flow speed 0.6 m/s.

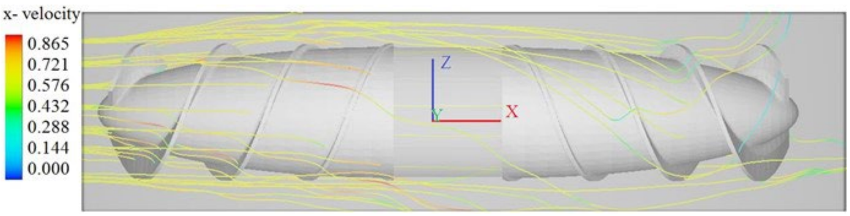


Fig. 3.4. Fluid flow lines around Durbis for flow speed 0.6 m/s.

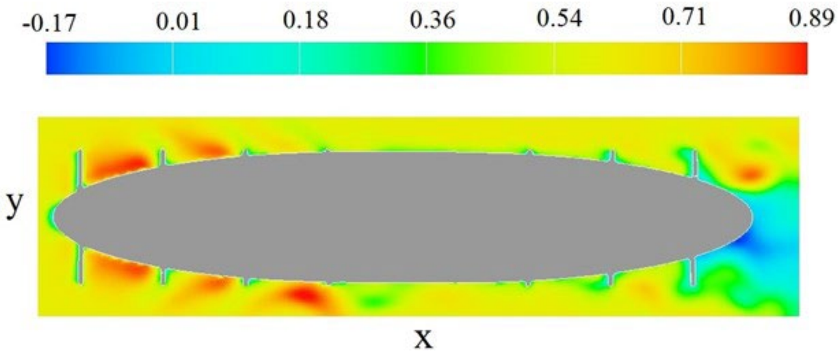


Fig. 3.5. Fluid speed contours in the x-y plane of the middle cross-section.

The software allows fixing Durbis in different positions, as well as rotate it during modelling, allowing to measure the main vector and moment of resistance forces. After these numerical experiments, quadratic approximation for linear and angular speed was used to obtain the variable coefficients, for example, DV_Kx and DV_KMx.

After creating the water resistance model, a moving spherical target was added to the mathematical model with an added force that moves it in three dimensions according to sinusoidal law $x(t) = -0.25\sin(0.5t)$, $y(t) = -0.25\cos(0.5t)$, $z(t) = -0.5\cos(1.5t)$, as shown in Fig. 3.6.

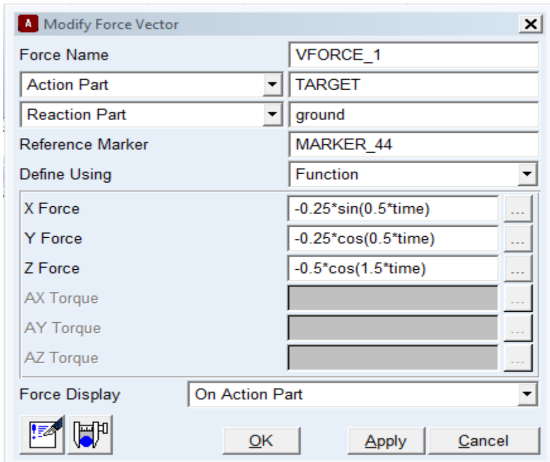


Fig. 3.6. Force functions for the target movement.

Figure 3.7 shows the model system with the target.

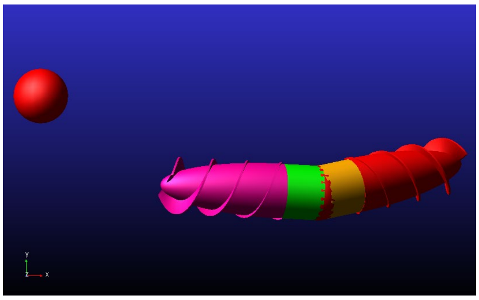

Fig. 3.7. Vehicle following a target.

In the initial state the vehicle is not bent, but, once the simulation starts, it assumes a direction in a moment of time and starts movement toward the target. The vehicle speed does not change significantly during the process of following the target, and, as shown in Fig. 3.9, it is constant within certain limits. The same applies to the distance to target. As time passes, approximately from the 20[th] second (Fig. 3.8), distance changes assume the same amplitude, meaning that the vehicle follows the target in a relatively stable way.

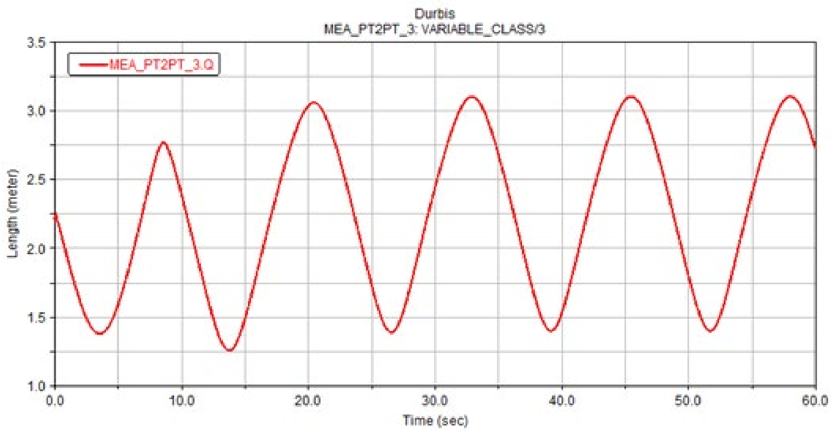


Fig. 3.8. Vehicle distance to target.

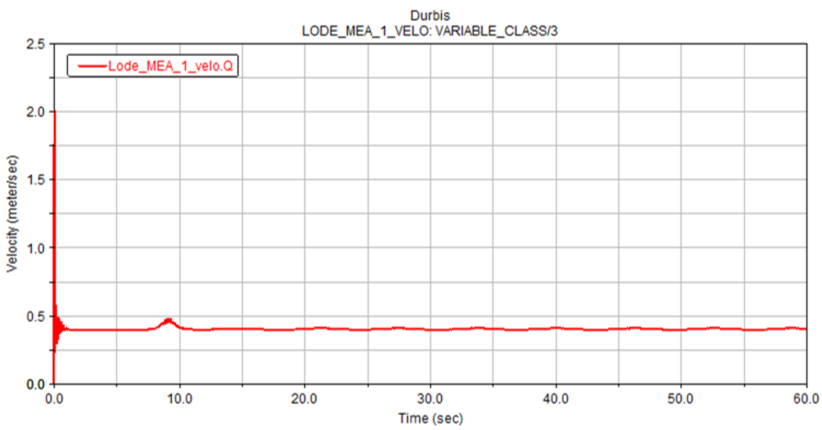


Fig. 3.9. Speed at which the vehicle follows the target.

# 4. MODELING DYNAMICS USING DIFFERENT CONTROL ALGORITHMS

The Durbis dynamics were modelled in the *MSC Adams* software. Forces that are characteristic for the flow environment were applied and defined for the model system, and movement laws were applied for the components, defining the control algorithms described earlier.

## 4.1. Development of the control principle for the helicoid vehicle

### 4.1.1. Description of the control algorithms

This section describes several control algorithms, for example, controlling direction, controlling speed, and kinematic control, trajectory planning. The appropriate control type is selected according to the environmental conditions where the vehicle operates, as well as the technical specifications of the vehicle itself.

When controlling direction, the task is to set a movement direction to the goal. In Fig. 4.1, vector $b$ is the object movement direction, while vector $a$ is the required direction, angle φ is the angular difference between these vectors and $k$ is the correction coefficient. These values can be related to torque in a general form:

$$\vec{T} = k(\vec{a} \times \vec{b}) = \frac{k^*}{\|a\|\|b\|} \cdot \vec{a} \times \vec{b} \qquad (4.1)$$

Operating with the torque, it would be possible to adjust the vectorial direction of the object, obtaining the required direction for attaining the goal or performing tracking. The control motors create an internal force moment. Expression (4.1) corresponds to the bow of the vehicle. Accordingly, the stern would then be subject to the opposite force moment $-\vec{T}$. The value of the force moment generated by both motors (vector norm) would be:

$$\|\vec{T}\| = k\|a\| \cdot \|b\| \cdot sin(\varphi) \qquad (4.2)$$

The purpose of the algorithm is to maintain a minimal deviation between the vectors, φ approaches the value of 0. This method would work well in conditions where there is no impact of external forces, for example, a river stream.

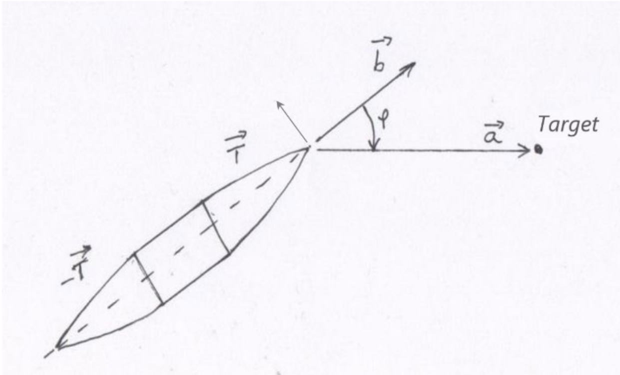


Fig. 4.1. Schematic depiction of controlling direction.

The principle for controlling speed is slightly different. The direction of the central axis of the object can be different from the direction of speed $v$, which is affected by some external factor, for example, the stream. This algorithm can be successfully applied in cases when the direction of the stream coincides with the vector of speed $v$ (see Fig. 4.2).

The algorithm can be described by the relation for torque $\vec{T}$:

$$\vec{T} = \frac{k}{\|a\|\|v\|} \cdot \vec{v} \times \vec{a} \tag{4.3}$$

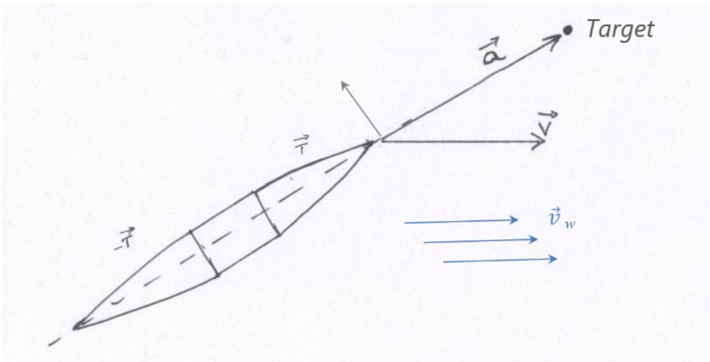


Fig. 4.2. Schematic depiction of controlling speed.

The kinematic model equations for the system do not include the actual forces that cause movement and the dynamical properties of the vehicle. This type of model allows separating the dynamics of the vehicle from its movement. In practice, both the motor torque and the turning angle or speed are implemented with a time offset. This means that the motor rotation at moment of time $t$ corresponds to the vehicle orientation at moment of time $t$-Δ, where Δ is time offset. When modelling such systems with universal multibody system simulation software, the simulation can be unstable because the rotation of the motor depends on orientation, which in turn depends on the motor rotation. This instability does not necessarily mean that the physical control system is unstable, although the possibility cannot be excluded.

The kinematic model of the underwater vehicle will be described using orthogonal coordinate systems – global coordinates ($O$, $X$, $Y$, $Z$) and local coordinates ($p$, $x$, $y$, $z$), as shown in Fig. 4.3.

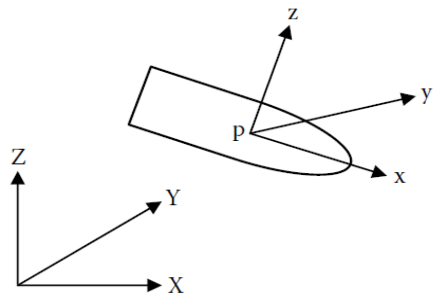


Fig. 4.3. Coordinate systems for the underwater vehicle.

The vehicle kinematics are described with six state variables and four input variables. The kinematic relations that describe the transformations of two coordinate systems may have several parametrizations. Here the Euler angle parametrization is used [15]. In the Euler angle depiction, the orientation of the inertial and local coordinate system is expressed with a sequence of three rotations – rolling $\Phi$, slope $\theta$, and deviation from route $\psi$, accordingly around the $x$, $y$ and $z$ axis.

After expressing different values and performing different transformations, a general form for the kinematic model is obtained:

$$\dot{q} = G(q)v \tag{4.4}$$

The equations described above correspond to the kinematic model of the system. The system is non-linear and does not follow an arbitrary trajectory in the vector space, meaning that the number of input factors for the system is less than the number of its states. The generalized speed vector $\dot{q}$ cannot assume independent values [1].

### 4.1.2. Generating the reference trajectory

The control algorithm described above may be classified as controlling from point to point or following a moving target. Higher level control systems also include trajectory planning [1], for example, moving around obstacles and predicting target movement. Algorithms of this level will not be reviewed in this paper.

### 4.1.3. Scheme for the controllable Durbis structure

In order to ensure the controllability of Durbis, a control principle similar to the motor rotation principle was employed, only in the case of Durbis rotation is applied to the threaded bodies, more precisely, only the front body which allows changing the direction of the propulsion force of the bow. Here it must be noted that the algorithm includes a correction for the turning engines in order to achieve movement of the bow in the required direction. But the turning engines generate internal torques, therefore the stern will turn in the opposite direction. The rotation of two parts will not be exactly the same because the water pressure on them is different.

This principle is achieved using a flexible middle part, its bending process in all the required directions is performed by a Cardan-type mechanism. This mechanism can be compared to a cross-type coordinate system where the bending pivots are placed around the *y* and *z* axis, as shown in Fig. 4.4. If torque $\vec{T}$ is applied to the propulsion threaded bodies, then the bow is subject to the moment $Q_y y$-$Q_z z$.

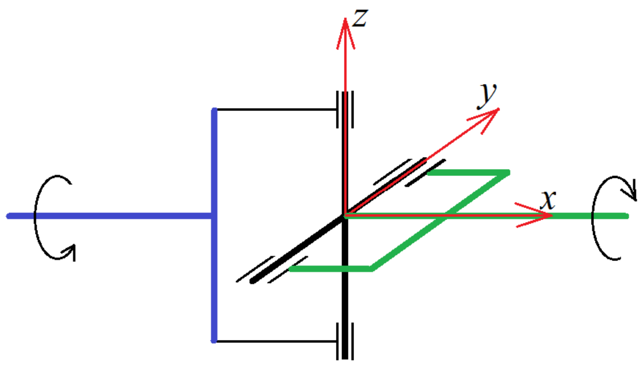


Fig. 4.4. Cross-type coordinate system.

Assuming that $\vec{a}$ is the target coordinate vector in projections in the cross-type coordinate system and $\vec{v}$ is the speed of the bow of Durbis (Fig. 4.2) in the cross-type coordinate, then the bow should be subjected to the aforementioned moment vector (4.3). But it is only possible to apply vector $Q_y y$-$Q_z z$. This means that is necessary to find $Q_y y$ and $Q_z z$ that ensure that the generated moment is as close to $\vec{T}$ as possible. Essentially this is solved simply by applying the $T_y$ projection in the pivot on the *y* axis and the $T_z$ projection in the pivot on the *z* axis.

#### 4.1.4. Stabilizing the middle body

Due to the unique design of Durbis, its middle part can freely rotate around the longitudinal axis of the vehicle. Taking into account the capacity of modern computers to rapidly process data, this does not cause great problems for the movement process of Durbis as an autonomous vehicle. But this problem may also be eliminated by adding a vertical direction sensor – gyro-accelerator using MEMS technology. The MEMS gyro-accelerator in combination with the *ArduinoUNO* microcontroller board creates a reference point that coincides with the cross-type middle part coordinate system or the Durbis Cardan-type mechanism coordinate system. This system electronically determines the direction of the centre axes of the model, their deviation from the coordinate axes of the physical system, labelled as $\Delta\varphi$. It is planned to compensate this value using the rotation force generated by one (or both) rotating threaded body. Figure 4.5 shows the aforementioned deviation of the coordinate axes $\Delta\varphi$ over the geometry of the vehicle. This idea has been borrowed from the inverted pendulum stabilization problem [16], described by equation

$$f(t) = k_1 x(t) + k_2 x'(t) + k_3(\theta(t) - \frac{\pi}{2}) + k_4 \theta'(t) \quad (4.5)$$

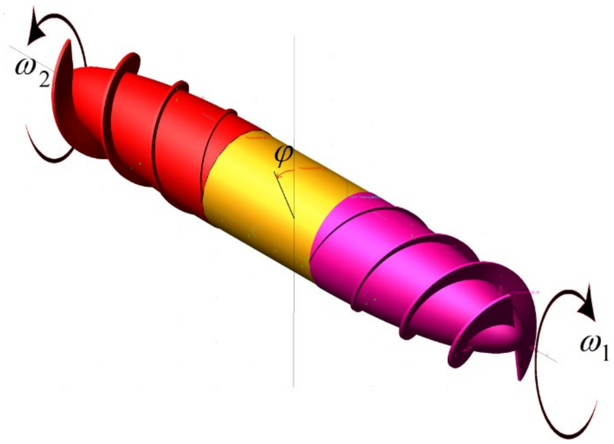


Fig. 4.5. Depiction of the principle of angular deviation of the vertical coordinate axis.

Given that our model may rotate around the *y* and *z* axes without affecting the vertical orientation of the middle part, compensation is only required for rotation around the longitudinal *x* axis of the model, or deviation from the *z* axis, as shown in Fig. 4.6. This condition makes our problem 1-dimension, as in the following equation:

$$f(t) = k_1\varphi(t) + k_2\varphi'(t) \tag{4.6}$$

The desired result is keeping the vehicle speed constant during displacement. Stabilization could be achieved by manipulating the projections of the threaded body rotation speeds $\Delta\omega_i$ over longitudinal axis of the Cardan-type mechanism coordinate system, with the following equation:

$$\begin{cases} \Delta\omega_1 = k_1\varphi + k_2\dfrac{\mathrm{d}\varphi}{\mathrm{d}t} \\ \Delta\omega_2 = -k_1\varphi - k_2\dfrac{\mathrm{d}\varphi}{\mathrm{d}t} \end{cases} \tag{4.7}$$

Manipulation of the rotation speeds of the threaded bodies could be achieved by equipping the turning motors for these bodies with proportionally integrated differential (PID) regulator control that would adjust the difference in rotation speeds of these motors for the bow and stern body.

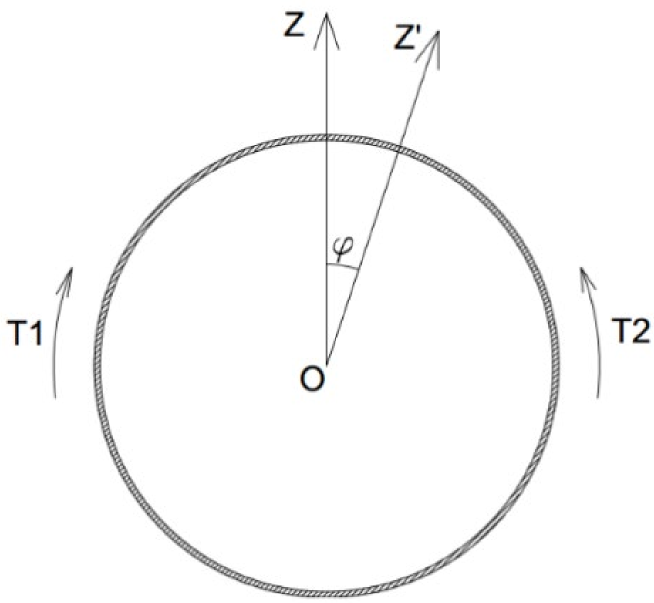


Fig. 4.6. Schematic depiction of the stabilization of the middle part, z-y cross-section.

### 4.1.5. Variants for the control algorithm

Bearing in mind that in further development Durbis could be an AUV, two variants for the control algorithm have been considered.

One of the variants is to implement a specific motor torque, allowing to control speed, which would allow adapting to swimming conditions in environments with variable or constant stream speed. Using this control algorithm, the underwater model could adapt and resist the dynamic influence of its environment in attaining its goal.

The second control algorithm that was considered is an implementation of the motor rotation angle that could be achieved using the functions offered by a step motor. In that case, in a given moment of time a rotation of the engine would be performed in the local coordinates of the model in order to adapt the vehicle movement course to the goal localized in global coordinates.

## 4.2. Controlling direction

An algorithm was modelled and reviewed where the mathematical model swims in space for 30 seconds, regulating its direction using a control motor. Figure 4.7 shows the placement of the vehicle and target in the *xy* global coordinate plane. The target moves the same as described before in Section 3.3 (Fig. 3.6).


Fig. 4.7. Placement of the objects in the *xy* coordinate plane.

When initiating movement, the vehicle comfortably assumes direction towards the target and approaches it within a couple of seconds, maintaining distance while precisely following the target. Figure 4.8 shows the vehicle speed graph.

The speed graph shows that at the start of the movement the vehicle quickly and without any jolts assumes a certain speed. After 7 seconds it increases speed, approaching the target at the same time, as can be seen in the graph in Fig. 4.9. This could be caused by sudden change of movement of the target after which the vehicle has successfully approached the target. After this period of instability, the vehicle maintains an essentially constant speed and the distance to the target somewhat increases, but a stable distance is maintained from now on.

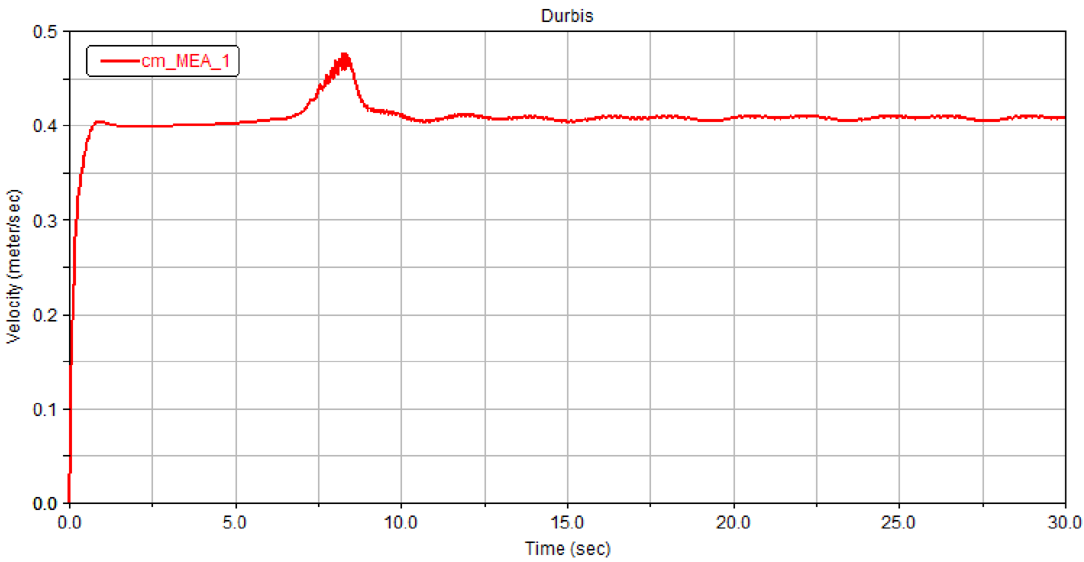


Fig. 4.8. Vehicle speed graph (controlling direction).

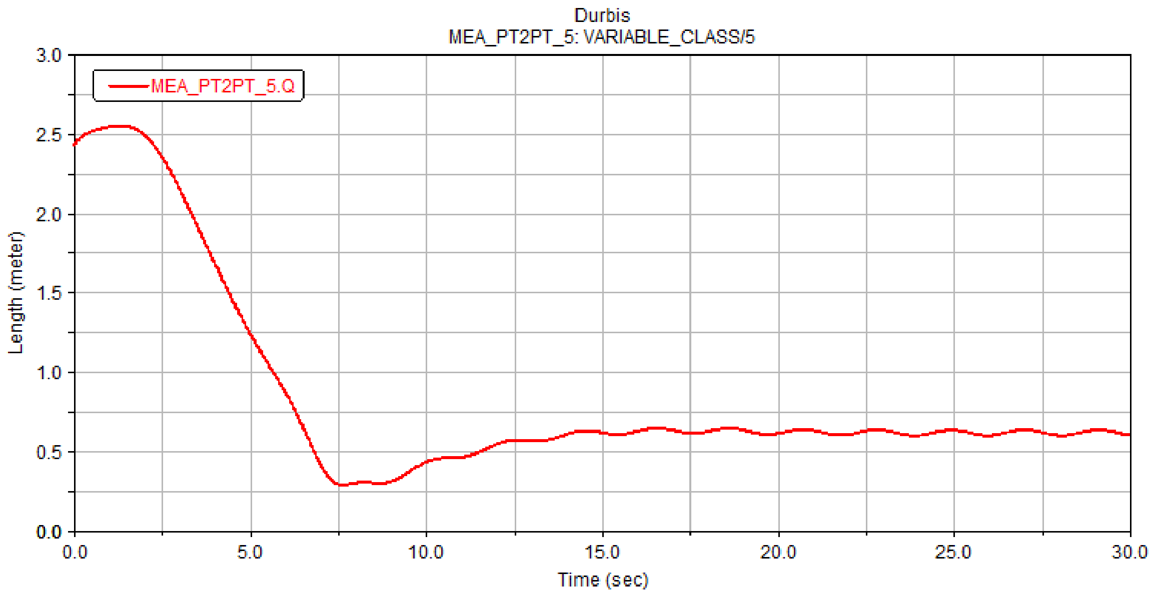


Fig. 4.9. Distance from vehicle bow to target.

## 4.3. Controlling speed

For comparing control algorithms, an algorithm for controlling speed was also created. The initial state of objects is the same that is shown in Fig. 4.7, their initial distance was not changed. The first observation is connected with the fact that the vehicle speed graph for this algorithm coincides with the vehicle speed for directional control that is shown in Fig. 4.8. It identically initiates movement, performs unstable speed change and then stabilizes.

However, the graph for the distance between the vehicle bow and target is significantly different. Figure 4.10 shows that the vehicle with this control algorithm cannot maintain a stable distance, it fluctuates in time. This is explained by the fact that the target object fluctuates in space, but the speed vector does not change its direction as rapidly, as a result the bow of the model does not assume the nearest state towards the target. Regardless, the average distance of the vehicle to the target does not change. It maintains a certain amplitude of distance change and does not fall behind from the target.

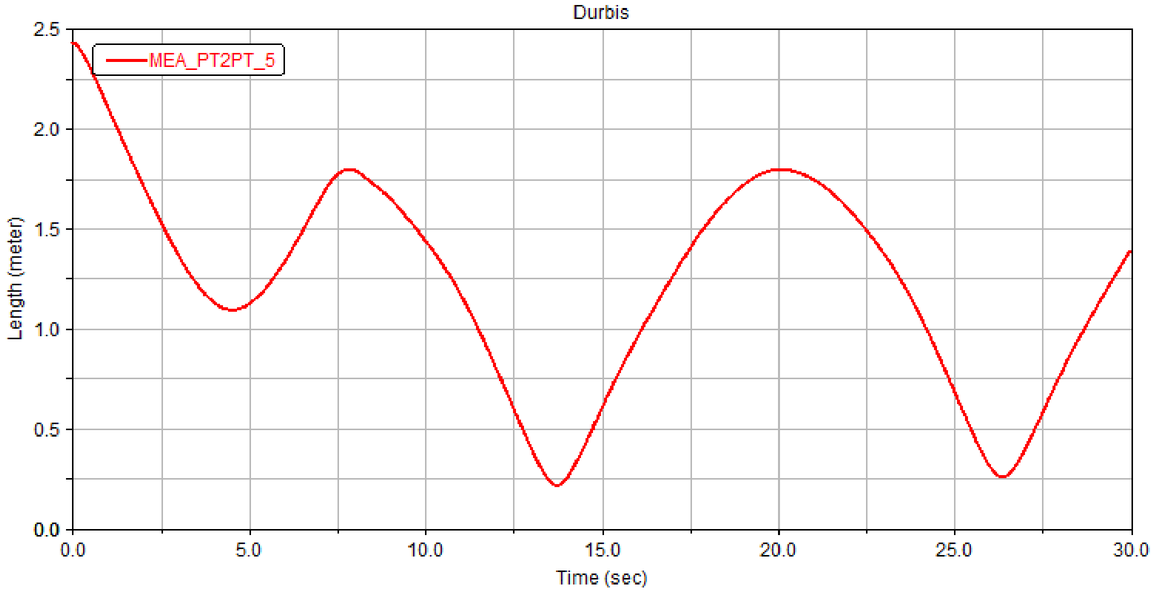


Fig. 4.10. Vehicle speed graph (controlling speed).

Figure 4.11 shows how the vehicle follows the target in separate moments of time.

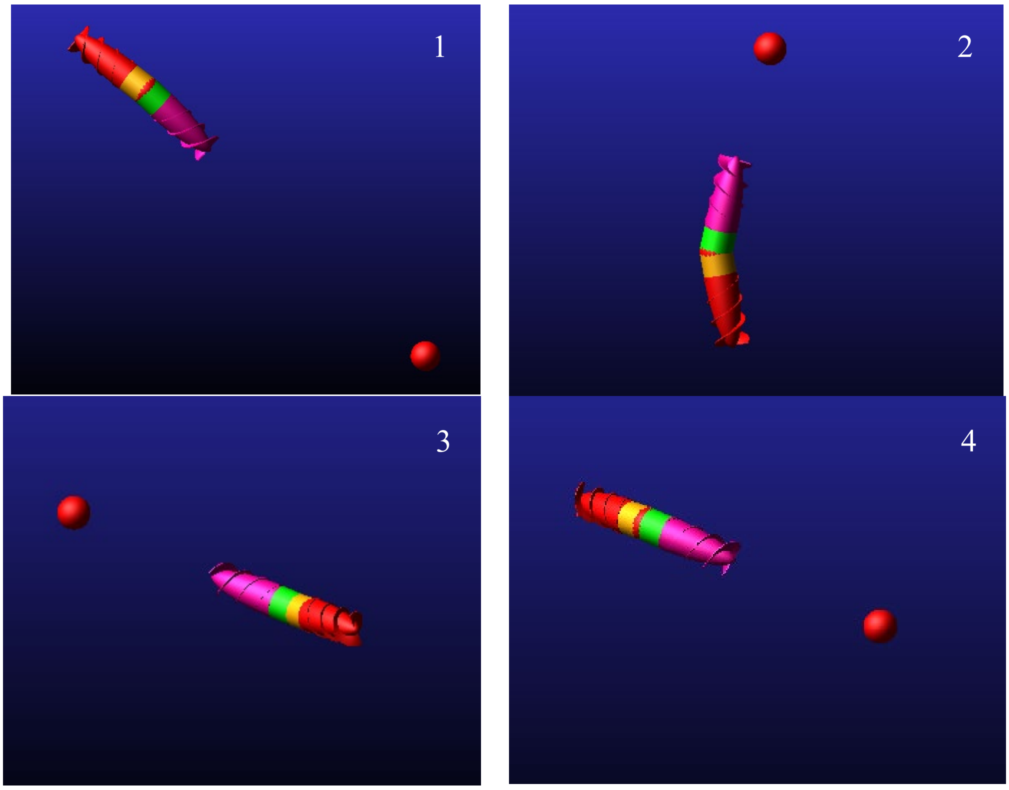


Fig. 4.11. Vehicle following the target at moments of time: 1) 5 s; 2) 10 s; 3) 20 s; 4) 26.5 s.

# 5. CREATING A MATHEMATICAL MODEL AND ANALYSING IT IN THE *EDEM* SOFTWARE

In order to assess the capacities of Durbis in a bulk environment, the discrete element modelling software *EDEM* was used in experiments. In simulation trials the model was created using an analogous method to the fluid environment models. The bulk substance flows in horizontal direction with an assigned flow speed $v = 0.6$ m/s. Gravitation is also acting, in a direction perpendicular to the flow. In order to simplify the simulation model, simple spherical particles were selected, approximately the size of a grain of wheat. The following properties were assigned to the particles: Poisson's ratio $v = 0.25$, solid substance density $\rho = 600$ kg/m$^3$ and shear module $G = 4\text{e} + 06$ Pa. The renewal rate and static friction ratio values were kept at the default values from the *EDEM* material model database, accordingly 0.55 and 0.2. In the physics section, in both cases – particle-particle and particle-geometry interaction – the Hertz-Mindlin (without sliding) contact model was used. The geometry of Durbis was placed in the calculation domain with enveloping particles, shown in Fig. 5.1.

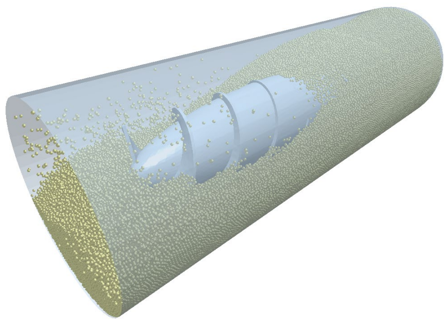

Fig. 5.1. Durbis in the simulation phase, where the calculation domain is filled with the discrete particles.

Seeing that there was no change of the flow state planned for the bulk environment, the same angular speed was defined for the bow and stern body.

A variable flow speed was defined for the particle flow, determining the moment when the speed of particles flowing in the intermediate space of the threads was approximately equal to the speed of particles in the environment. Figure 5.2 shows this moment of time. The flow occurs in the positive direction of the *x* axis. At this moment the established flow speed is 0.4 m/s, the defined thread body rotation speed $\omega = 35$ rad/s.

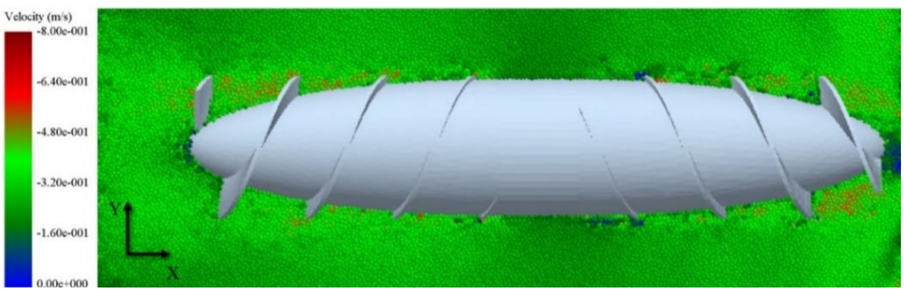


Fig. 5.2. Durbis in the flow of discrete particles, *EDEM* simulation.

# 6. MODEL PROTOTYPE

A prototype of Durbis with control functions was created. The control for Durbis was implemented with a flexible middle body that can be bent using a system of pivots that is used for controlling kites. This system in principle is based on the idea of a Cardan-type mechanism fastening, where one part allows movement in direction up-down, and the other – sideways, and the parts are connected to each other (see Fig. 6.1).

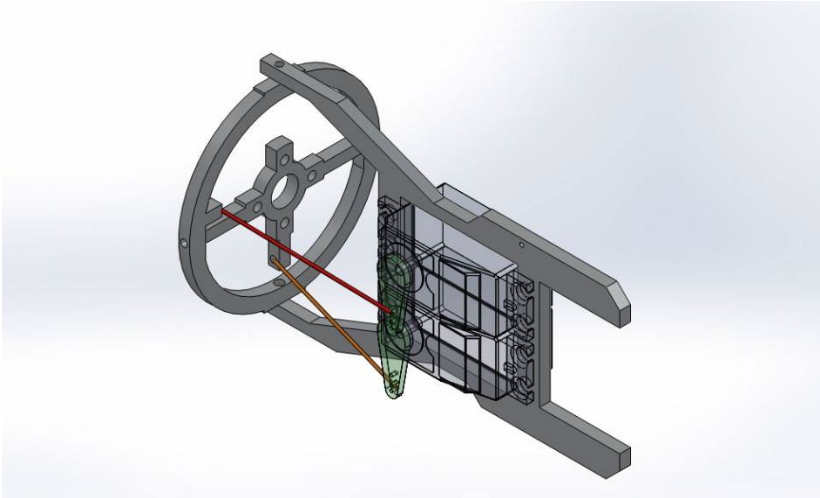

Fig. 6.1. Cardan-type control mechanism.

For the Durbis protype, the external control ring that is attached to a stationary frame is used for changing direction sideways, while the middle part that is attached to the external ring is used for vertical direction change. Both of these components are controlled with servomotors that are sent an analog signal from the remote control. Special low-profile servomotors were selected to save space in the middle body that is required for the 11.1 V battery, the propulsion motor controller and a 4 channel receiver. The mechanism was manufactured from 4 mm thick EN AW-5754 using laser cutting technology.

The other model body components were manufactured using 3D printing. The assembled Durbis is shown in Fig. 6.2.

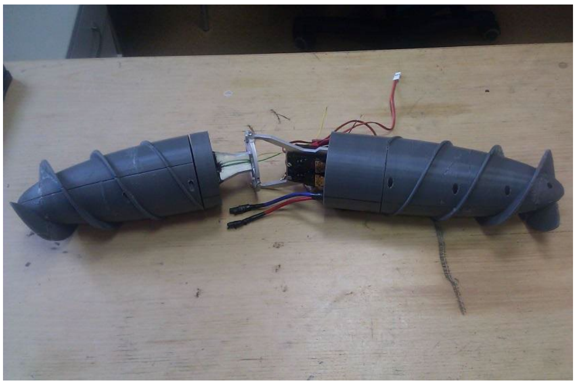

Fig. 6.2. Durbis in an assembled state, without the silicon shell.

After conducting tests in a water reservoir, as shown in Fig. 6.3, it was observed that under water Durbis is capable of swimming approximately the total length of its body in a single second, which is approximately 60 cm/s, at the threaded body rotation speed ~10 revolutions per second. In experiments carried out in a lake, Durbis was even capable of jumping above the surface of the water, see Fig. 6.4.

Fig. 6.3. Durbis in water with an additional mass.

Fig. 6.4. Durbis jumping out of water.

# CONCLUSIONS

The following conclusions can be drawn from the results:

1. The proposed vehicle propulsion principle that was initially developed for using under water is similar to the movement principle of bacteria *Salmonella typhimurium,* although it is different in that the rotating bow also creates additional propulsion force. From the technical point of view, the proposed principle is original and currently has not been implemented in under water or any other vehicles.
2. In order to perform the spatial modelling of the mechanism and fluid dynamics, a metamodeling principle was developed – modelling experiments were performed with CFD software, as a result of which water resistance models were created. The water resistance models were implemented in the multibody dynamics modelling software *MSC.Adams*. Validation with the natural prototype fully confirmed the adequacy of the mathematical model. The prototype allowed performing maneuvers in a real water reservoir without losing performance at any point and maintaining a constant speed – approximately 0.6 m/s, which coincides with the *Flow3D* mathematical model results. Given that the speed of natural prototype was determined approximate, by visual method, 5–10 % deviation from modelled results is presumed as possibility. In verification between *Flow3D* and *MSC Adams* movement speed results showed 33 % difference – target tracking speed 0.4 m/s.
3. The developed kinematic scheme with a flexible middle part and control of bending motors confirmed the performance when simulating the vehicle dynamics in the flow modelling software *Flow3D*, discrete element modelling software *EDEM* and the multibody dynamics analysis software *MSC Adams*.
4. A physical prototype of the vehicle was created using modern technology: CAD software *SolidWorks, Flow3D, EDEM,* and *MSC Adams.* Mathematical modelling and physical prototype tests fully confirmed the performance and efficiency of the proposed principle of propulsion. At a relatively low motor power and torque in water, a fairly high movement speed can be achieved – 0.6 m/s. The speed in bulk environment is 0.4 m/s.
5. This principle of propulsion can be applied to autonomous unmanned vehicles moving in fluids or bulk environments. If the body and threads are made from a flexible material, the vehicle can move through pipes. A mechanism of micro-size could also be used in medicine, moving through blood vessels and performing medical manipulations. If the flexible middle body could be made from artificial muscle tissue, the existing mechanisms of the middle body (mainly the two servomotors) could be dispensed with, saving space for other important components. If the body and threads are made from materials that have high wear resistance and low friction resistance against rock, the vehicle could drill underground, performing the required manipulations, or perform rescue work in case of cave-ins or landslides.
6. Further directions for study should concentrate on the control of such vehicles, creating, for example, a piezoelectric change of the front thread profile in order to perform

movement direction change. Comprehensive study is required for the optimization of the bow and stern propulsion thread form in order to achieve maximum speed, maneuverability and energy efficiency. If the vehicle is equipped with a suitable energy source, the design has potential for performing operations on other planets.

7. Two PD-type algorithms have been created for following a moving target. Mathematic modelling confirmed the efficiency of the algorithms.
8. Further research is required to determine the most suitable control principle for the developed propulsion system in different conditions. It is necessary to implement the described principle for stabilizing the rotation of the middle part. However, this aspect is not critical for autonomous unmanned vehicles, since modern computer systems are capable of sufficiently rapid recalculation of coordinate system data in order to prevent system confusion and maintain course. In situations where the device is incapable of directly communicating with the mission centre through GPS or any other antenna located nearby, autonomous navigation systems are applied, which for underwater vehicles mainly consist of acoustic positioning and inertial navigation systems. In other media, such methods as the Monte Carlo localization and parallel localization and mapping can be applied.

# BIBLIOGRAPHY


1. Wadoo S., Kachroo P., *Autonomous underwater vehicles: modeling, control, design, and simulation*. Taylor and Francis Group, LLC, 2011.
2. KEMPCO INC. *Amphibious land reclamation vehicle*. Peter Kovacs, Mihaly Kovacs, Endro Kovacs (inventors). US Cl. US5509370A. Publ. 1996-04-23.
3. Shardcore, "e coli (2006)", http://www.shardcore.org/shardpress2019/2006/01/19/e-coli-2006/. Accessed: 14.09.2021.
4. Kon K., "Treponema pallidum, spirochetes bacteria that cause syphilis, 3D illustration", https://www.shutterstock.com/image-illustration/treponema-pallidum-spirochetes-bacteria-that-cause-783390835. Accessed: 14.09.2021.
5. Weymouth G. D., Triantafyllou M. S. Ultra-fast escape of a deformable jet-propelled body. *Journal of Fluid Mechanics*, 721:367{385, 2013.
6. Vincent J. F. V. et al. Biomimetics: its practice and theory. *Journal of the Royal Society Interface*. 22 August 2006, **3** (9), pp. 471–482. doi:10.1098/rsif.2006.0127. PMC 1664643. PMID 16849244.
7. Toda Y., Rahman Md. M., Hashimoto S., Mino J. Development of the Osaka University Squid-Like Underwater Robot, In: *10th Symposium on High-Performance Marine Vehicles HIPER'16*, Italy, Cortona, 17–19 October 2016. Cortona: 2016, pp. 283–296.
8. Huffard, C. L. Locomotion by abdopus aculeatus (cephalopoda: Octopodidae): walking the line between primary and secondary defenses. *J. Expl. Biol.*, 209:3697{3707, 2006.
9. Weymouth G. D., Biologically Inspired Force Enhancement for Maritime Propulsion and Maneuvering, In: *10th Symposium on High-Performance Marine Vehicles HIPER'16*, Italy, Cortona, 17–19 October 2016. Cortona: 2016, pp. 401–414.
10. Triantafyllou M. S., Weymouth G. D., Miao J. Biomimetic survival hydrodynamics and flow sensing. *Annual Review of Fluid Mechanics*, 48(1):null, 2016. doi: 10.1146/annurev-fluid-122414-034329.
11. "FILOSE research project", http://www.filose.eu/. Accessed: 06.03.2021.
12. International Submarine Engineering Ltd., "EXPLORER AUTONOMOUS UNDERWATER VEHICLE (AUV)", https://auvac.org/files/uploads/platform_pdf/ise%20explorer%202009_2.pdf. Accessed: 10.03.2021.
13. International Submarine Engineering Ltd., "Explorer AUV", https://ise.bc.ca/product/explorer/. Accessed: 10.03.2021.
14. Carroll, J., Marcum, D. Developing a Surrogate-Based Time-Averaged Momentum Source Model from 3D CFD Simulations of Small-Scale Propellers. *Lecture Notes in Engineering and Computer Science: Proceedings of The World Congress on Engineering*, London, United Kingdom, July 2013, pp. 1622–1627, (2013).
15. Sordalen O. J., Dalsmo M., Egeland O. An exponentially convergent law for a nonholonomic underwater vehicle, in *1993 IEEE International Conference on Robotics and Automation,* Atlanta, GA, May 2–7, 1993, 790–795.

**16.** Gäfvert M. Modelling the Furuta Pendulum. Department of Automatic Control, Lund Institute of Technology (LTH), 1998. (Technical Reports TFRT-7574).

**Mārcis Eimanis** was born in 1990 in Saldus. He obtained a Bachelor's degree in Mechanical Engineering (2012) and a Master's degree in Mechanics and Mechanical Engineering (2014) from Riga Technical University. From 2013 to 2017, he worked in the metal processing company EHT Fabrik Ltd, holding the position of an engineer. From 2017 to 2021, he worked in Skonto Plan LTD as a production engineer, at the same time, from 2019 to 2021, holding the position of a research assistant at the Riga Technical University and participating in a Latvian research project.
Currently, Mārcis Eimanis is a mechanical engineer at Giraffe360 Ltd.